

# SRI International

AD-A280 094



---

Quarterly Technical Report 7 • 3 June 1994

## IR MATERIALS PRODUCIBILITY

A. Sher, Program Director  
M.A. Berding, Sr. Research Physicist  
A.T. Paxton, Research Physicist  
Physical Electronics Laboratory

M.W. Muller, Consultant

SRI Project 3820

Prepared for:

Contracting Officer's Technical Representative  
Advanced Research Projects Agency  
Microelectronics Technology Office (MTO)  
3701 N. Fairfax Drive  
Arlington, VA 22203-1714

Attn: Mr. Raymond Balcerak

ARPA Order No. 8557; Program Code Nos. 2H20, 2D10

Contract MDA972-92-C-0053

Covering the period: 1 February through 30 April 1994



94-17313  
12P8

The views and conclusions contained in this document are those of the authors and should not be interpreted as representing the official policies, either expressed or implied, of the Advanced Research Projects Agency or the U.S. Government.

APPROVED FOR PUBLIC RELEASE  
DISTRIBUTION UNLIMITED

94 6 7 070

## IR MATERIALS PRODUCIBILITY

A. Sher, Program Director  
M.A. Berding, Sr. Research Physicist  
A.T. Paxton, Research Physicist  
Physical Electronics Laboratory

M.W. Muller, Consultant

SRI Project 3820

Prepared for:

Contracting Officer's Technical Representative  
Advanced Research Projects Agency  
Microelectronics Technology Office (MTO)  
3701 N. Fairfax Drive  
Arlington, VA 22203-1714  
Attn: Mr. Raymond Balcerak

Accesion For	
NTIS	CRA&I
DTIC	TAB
Unannounced	
Justification	
By _____	
Distribution /	
Availability Codes	
Dist	Avail and/or Special
A-1	

ARPA Order No. 8557; Program Code Nos. 2H20, 2D10

Contract MDA972-92-C-0053

Covering the period: 1 February through 30 April 1994

The views and conclusions contained in this document are those of the authors and should not be interpreted as representing the official policies, either expressed or implied, of the Advanced Research Projects Agency or the U.S. Government.

APPROVED FOR PUBLIC RELEASE  
DISTRIBUTION UNLIMITED

Approved:

Eric Pearson, Director  
Physical Electronics Laboratory

Donald L. Nielson, Vice President  
Computing and Engineering Sciences Division

**REPORT DOCUMENTATION PAGE**Form Approved  
OMB No. 0704-0188

Public reporting burden for this collection of information is estimated to average 1 hour per response, including the time for reviewing instructions, searching existing data sources, gathering and maintaining the data needed, and completing and reviewing the collection of information. Send comments regarding this burden estimate or any other aspect of this collection of information, including suggestions for reducing this burden, to Washington Headquarters Services, Directorate for Information Operations and Reports, 1215 Jefferson Davis Highway, Suite 1204, Arlington, VA 22202-4302, and to the Office of Management and Budget, Paperwork Reduction Project (0704-0188), Washington, DC 20503.

1. AGENCY USE ONLY (Leave Blank)	2. REPORT DATE	3. REPORT TYPE AND DATES COVERED	
	3 June 1994	Quarterly Technical 7 (1 Feb. to 30 April 1994)	
4. TITLE AND SUBTITLE		5. FUNDING NUMBERS	
IR Materials Producibility			
6. AUTHORS			
A. Sher, M.A. Berding, A.T. Paxton, SRI International M. Muller, Consultant			
7. PERFORMING ORGANIZATION NAME(S) AND ADDRESS(ES)		8. PERFORMING ORGANIZATION REPORT NUMBER	
SRI International 333 Ravenswood Avenue Menlo Park, CA 94025-3493			
9. SPONSORING/MONITORING AGENCY NAME(S) AND ADDRESS(ES)		10. SPONSORING/MONITORING AGENCY REPORT NUMBER	
Advanced Research Projects Agency Microelectronics Technology Office, Infrared Focal Plane Array Program 3701 North Fairfax Drive Arlington, Virginia 22203-1714			
11. SUPPLEMENTARY NOTES			
12a. DISTRIBUTION/AVAILABILITY STATEMENT		12b. DISTRIBUTION CODE	
Approved for public release; distribution unlimited			
13. ABSTRACT (Maximum 200 words)			
The formation energy for mercury vacancy - tellurium antisite pairs is calculated. We developed a method for calculating the ionization energies of the defects in semiconductors. The electron-phonon interaction-induced band-edge shifts in semiconductors are calculated using accurate band structures. The temperature variation of gaps in GaAs (done to validate our method) and Hg <sub>0.78</sub> Cd <sub>0.22</sub> Te have been calculated and are found to agree well with experiments.			
14. SUBJECT TERMS		15. NUMBER OF PAGES	
native point defect; defect density; photonic material; IRFPA; HgTe; CdTe; ZnSe; HgCdTe; LiNbO <sub>3</sub>		12	
		16. PRICE CODE	T
17. SECURITY CLASSIFICATION OF REPORT	18. SECURITY CLASSIFICATION OF THIS PAGE	19. SECURITY CLASSIFICATION OF ABSTRACT	20. LIMITATION OF ABSTRACT
Unclassified	Unclassified	Unclassified	Unlimited

## SUMMARY

The work summarized in this report covers the seventh quarter of a program with a goal that is threefold: first, to study the properties of native point defects in infrared focal-plane array (IRFPA) active and substrate materials; second, to study the properties of native point defects in two classes of photonic materials, the wide-gap II-VI compounds (ZnSe as the prototype for which impurity properties will also be calculated) and the nonlinear optical materials (LiNbO<sub>3</sub> as the prototype); and third to study the properties of HgZnTe as a very-long-wave infrared (VLWIR) detector material. Our accomplishments in the seventh quarter include

- Beginning of calculation of the tellurium antisite - mercury vacancy pair. Preliminary results indicate that these complex concentrations will be high enough to impact device performance. They serve as reservoirs of Te<sub>Hg</sub>, which keeps the concentrations of these donors high in commonly used annealing procedures, and the complexes plus the Te<sub>Hg</sub> may account for the Shockley-Read centers that currently limit FPA performance at intermediate operating temperatures. Annealing procedures to eliminate the adverse effects of these defects are being formulated.
- Continued calculation of the defect ionization energies in CdTe, ZnSe, and LiNbO<sub>3</sub>.
- Calculation of the temperature dependent band gap of semiconductors. Our calculation predicts the temperature variations of the band gaps and band offsets of HgCdTe, GaAs, InSb, InAs, and InP correctly. The band offset between HgTe and CdTe varies from 350 meV at T=0 to 215 meV at 300 K. This will modify the heterojunction designs for devices intended to operate at elevated temperatures.

Accesion For	
NTIS	CRA&I <input checked="" type="checkbox"/>
DTIC	TAB <input type="checkbox"/>
Unannounced <input type="checkbox"/>	
Justification .....	
By .....	
Distribution /	
Availability Codes	
Dist	Avail and / or Special
A-1	

## **CONTENTS**

<b>1</b>	<b>NATIVE POINT DEFECTS IN HgCdTe AND RELATED IR MATERIALS</b>	<b>1</b>
1.1	MERCURY VACANCY TELLURIUM ANTISITE COMPLEX . . . . .	1
1.2	NATIVE POINT DEFECTS IN CdTe . . . . .	1
1.3	TEMPERATURE-DEPENDENT BAND GAP . . . . .	1
<b>2</b>	<b>HgZnTe AS AN LWIR DETECTOR MATERIAL</b>	<b>1</b>
<b>3</b>	<b>WIDE-GAP II-VI COMPOUNDS (ZnSe AS THE PROTOTYPE)</b>	<b>2</b>
<b>4</b>	<b>NONLINEAR OPTICAL MATERIALS (LiNbO<sub>3</sub> AS THE PROTOTYPE)</b>	<b>2</b>
<b>5</b>	<b>WORK PLANNED</b>	<b>2</b>

## **1. NATIVE POINT DEFECTS IN HgCdTe AND RELATED IR MATERIALS**

### **1.1 MERCURY VACANCY TELLURIUM ANTISITE COMPLEX**

We have continued to calculate the formation energy for the mercury vacancy tellurium antisite pair. The revised calculations will include the relaxation of the two defects. Once the formation energy is calculated, we will revise our estimates of the density of this defect and its impact on device properties.

### **1.2 NATIVE POINT DEFECTS IN CdTe**

We worked on a method for calculating the ionization energies of the defects in semiconductors. While we were able to assume that the ionization energies of donors and acceptors are zero in HgCdTe because of its small band gap, we cannot do this for CdTe.

### **1.3 TEMPERATURE-DEPENDENT BAND GAP**

The electron-phonon interaction-induced band-edge shifts in semiconductors are calculated using accurate band structures. The temperature variation of gaps in GaAs (done to validate our method) and  $Hg_{0.78}Cd_{0.22}Te$  (MCT) have been calculated and are found to agree well with experiments. While the simple picture that the intra (inter)-band transitions reduce (increase) the gap still holds, we have shown that both the conduction band edge  $E_c$  and valence band edge  $E_v$  move down in energy. These large shifts in  $E_v$  can affect the valence band offsets in heterojunctions at finite temperature. Detailed band-to-band analysis explains why the gap in InSb decreases with T, whereas it increases in MCT alloys with a comparable band gap. A paper on this work (included here as the Appendix) has been submitted to *Physical Review Letters*.

## **2. HgZnTe AS AN LWIR DETECTOR MATERIAL**

We have completed the calculation of the band structure of  $Hg_{1-x}Zn_xTe$  as a function of  $x$  using a hybrid pseudopotential tight-binding method. This method has been applied extensively to a wide range of group IV, III-V, and II-VI compounds and alloys<sup>†</sup> with a great degree of success. The method uses a generic pseudopotential for all of the semiconductors to which a tight-binding Hamiltonian is added as a perturbation. The parameters of the tight-binding Hamiltonian are chosen empirically so as to give good agreement with the experimental band structure. The coherent potential approximation (CPA) is used to calculate the alloy band structure from those of the constituent compounds.

---

<sup>†</sup> A.-B. Chen and A. Sher, "The theory of semiconductor alloys", unpublished.

### **3. WIDE-GAP II-VI COMPOUNDS (ZnSe AS THE PROTOTYPE)**

Our work has continued on the calculation of the ionization energies of the defects in ZnSe.

### **4. NONLINEAR OPTICAL MATERIALS (LiNbO<sub>3</sub> AS THE PROTOTYPE)**

This quarter our work has continued on the calculation of the ionization energies of the defects in LiNbO<sub>3</sub>.

### **5. WORK PLANNED**

In the next quarter we will continue the calculation of the ionization energies of the defects in CdTe, ZnSe, and LiNbO<sub>3</sub>, and the incorporation of these energies into the quasichemical formalism to predict densities of the ionized defect concentrations. We expect to complete the calculation of the binding energy of the tellurium antisite mercury vacancy pair. We will be calculating the transport properties of HgZnTe, including the electron and hole mobilities and the Hall coefficient and carrier concentration as a function of  $x$ , T, N<sub>D</sub>, and N<sub>A</sub>.

## **APPENDIX**

# Temperature dependence of band gaps in semiconductors

Srinivasan Krishnamurthy<sup>a</sup>, A.-B. Chen<sup>b</sup>, and A. Sher<sup>a</sup>

<sup>a</sup> SRI International, Menlo Park, CA 94025

<sup>b</sup> Physics Department, Auburn University, Auburn, AL 36849

(May 25, 1994)

The electron-phonon interaction-induced band-edge shifts in semiconductors are calculated using accurate band structures. The calculated temperature variation of gaps in GaAs and  $Hg_{0.78}Cd_{0.22}Te$ (MCT) agrees well with experiments. While the simple picture that the intra(inter)-band transitions reduce (increase) the gap still holds, we show that both the conduction band edge  $E_c$  and valence band edge  $E_v$  move down in energy. These large shifts in  $E_v$  can affect the valence band offsets in heterojunctions at finite temperature. Detailed band-to-band analysis explains why the gap in InSb decreases with T, whereas it increases in MCT alloys with a comparable band gap.

PACS numbers 63.20.Kr, 71.25.Tn

The temperature (T) dependence of energy gaps of semiconductors is of great physical and technological interest. Numerous theoretical [1-9] and experimental [10-19] studies have been undertaken to obtain both qualitative and quantitative variations of various gaps in semiconductors. While the gap decreases with increasing temperature in medium-gap and wide-gap semiconductors, it increases in small-gap materials such as HgCdTe, PbS, PbSe, and PbTe. The temperature variation is usually attributed to two causes: thermal expansion of the lattices and electron-phonon interactions. Thermal expansion always reduces gaps. Here we show, starting from accurate band structures and wave functions, from proper phonon dispersion relations, and taking account of matrix elements of the electron-phonon interactions, that the calculated gap variations in GaAs and  $Hg_{0.78}Cd_{0.22}Te$  agree well with experiments. In a perturbation-theory treatment of electron-phonon interactions, the intra-band transitions reduce the gap whereas interband transitions increase it, and the net shift in the gap can be positive or negative. We show that while this simple physical picture is still valid, both conduction and valence band edges move down in energy. When the valence band edge moves more than the conduction band edge, the gap increases with T as in the case of  $Hg_{0.78}Cd_{0.22}Te$ . The reverse occurs for GaAs and most other semiconductors. This observation has an important effect on our understanding of the variation of band offsets in semiconductor heterojunctions. The contributions from each phonon branch to each electron band have been obtained to assist physical understanding of the underlying causes of the variations.

Our calculation of the temperature dependence of the band gap starts with accurate band structures. Empirical pseudopotential form factors are used to construct a hybrid tight-binding (HTB) Hamiltonian in a minimum set of  $sp^3$  Slater orbitals per atom. This Hamiltonian is then transformed into an orthonormal basis. A site-diagonal

spin-orbit Hamiltonian and a perturbative Hamiltonian are added to fine-tune the band structures to agree well with experiments [20,21]. Various results obtained using these band structures are found to be quite reliable [21-23]. This treatment tests the accuracy of the wave functions as well as the energies.

The dilation contribution to the band gap reduction is given [5,9] by  $3 \alpha_T B \delta E_g / \delta P$ , where the thermal expansion coefficient of the lattice  $\alpha_T$ , the bulk modulus B, and the change in the gap with pressure are obtained from the literature [19]. The electron-phonon interactions that cause the band structures to change are treated in perturbation theory. The total potential is assumed to be a sum of potentials from single atoms. The atomic potential in the solid is traditionally expanded in a Taylor series with only the leading term retained, and the energy is evaluated in a second-order perturbation theory commonly known as a self energy correction. However, it has been demonstrated by a number of researchers [3,4,6] that retention of first-order perturbation terms with a second term in Taylor series is necessary to preserve symmetry. We retain both terms. The change in the energy at a given wave vector  $k$  is

$$\Delta E_{nk} = \langle nk | V_2 | nk \rangle + \sum_{n'k'} \frac{|\langle n'k' | V_1 | nk \rangle|^2}{E_{nk} - E_{n'k'}} \quad (1)$$

where  $V_1$  and  $V_2$  are the first two terms in the Taylor expansion of the total potential in powers of atomic displacements  $\xi$ . In the TB formalism, Eq. (1) can be written in terms of

$$\langle l'j'\alpha' | V_1 | l'j\alpha \rangle = \nabla V_{\alpha\alpha'}(d_{ll'}^{jj'}) \cdot (\xi_{l'j'} - \xi_{lj}), \quad (2)$$

and

$$\begin{aligned} \langle l'j'\alpha' | V_2 | l'j\alpha \rangle = & \frac{1}{2} [\xi_{l'j'} \cdot (\nabla)^2 V_{\alpha\alpha'}(d_{ll'}^{jj'}) \cdot \xi_{l'j'} \\ & + \xi_{lj} \cdot (\nabla)^2 V_{\alpha\alpha'}(d_{ll'}^{jj'}) \cdot \xi_{lj}], \end{aligned} \quad (3)$$

where  $d_{ll'}^{jj'}$  is the position vector connecting atomic sites l, species (anion or cation) j and site l', species j', and  $V_{\alpha\alpha'}(d_{ll'}^{jj'})$  is a HTB matrix element between the orbitals  $\alpha$  and  $\alpha'$  located on those atoms. From quantum theory of harmonic crystals, the atomic displacements  $\xi$  can be expressed in terms of normal modes of phonons. We have

$$\xi_{ij} = [\frac{M}{3NM_j}]^{\frac{1}{2}} \sum_{q,\lambda} \omega_{\lambda q}^{-\frac{1}{2}} [e_{\lambda q}^j a_{\lambda q} e^{iq \cdot (l+r_j)} + e_{\lambda q}^{*j} a_{\lambda q}^\dagger e^{-iq \cdot (l+r_j)}] \quad (4)$$

where  $q$  and  $\omega$  are phonon wave vector and frequency,  $\lambda$  denotes phonon branch,  $a(a^\dagger)$  is the phonon annihilation (creation) operator,  $M$  is the atomic mass and  $e$  is an eigenvector of the six-dimensional eigenvalue problem:

$$M\omega^2 e = D(q)e \quad (5)$$

Evaluation of the matrix elements given by Eqs. (2) and (3) requires knowledge of spatial variations of the interatomic TB matrix elements  $V_{\alpha\alpha'}$ . In Harrison's universal TB approach [24], these matrix elements scale as  $d^{-2}$ . In our generalization, we assume that  $V_{\alpha\alpha'}$  varies as  $d^{-m}$  and the repulsive first-neighbor pair energy, following Harrison's overlap argument, as  $\eta/d^{2m}$ . The two unknowns  $m$  and  $\eta$  are determined by requiring that the calculated equilibrium bond length and bulk modulus agree well with experiments. This approach, with electrons and phonons treated from the same underlying Hamiltonian, has previously been used successfully to explain hot electron transistor characteristics [23] and is also in fairly good agreement with first-principles calculations [25]. The dynamical matrix  $D$  is calculated from the valence force field model [26].

The calculational procedure is as follows. For a chosen material,  $m$  and  $\eta$  are evaluated. Then the first and second derivatives of all interatomic matrix elements are

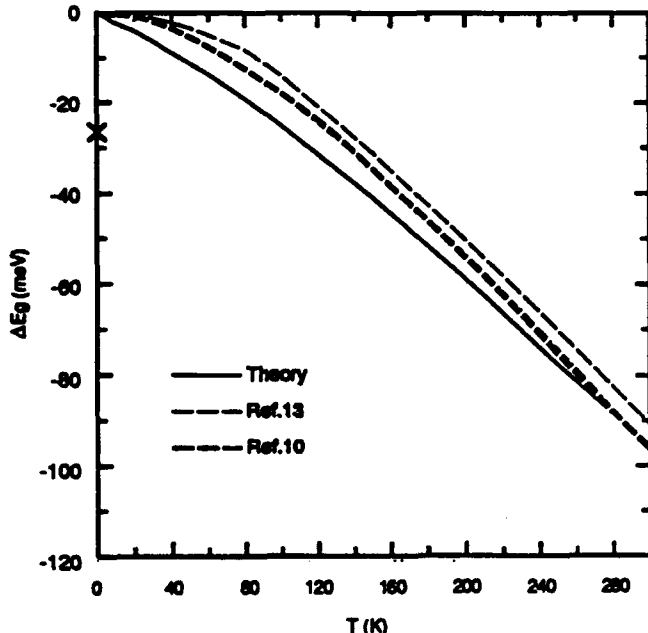


FIG. 1. Change in the band gap of GaAs with temperature.

obtained. The dynamical matrix is diagonalized to obtain  $\omega$  and  $e$  as a function of  $q$  and  $\lambda$ . The phonon structures and electronic band structures are used [Eqs. (1) through (4)] to obtain the change in the band energy at a given  $k$ . The polar coupling terms are included in the longitudinal optical phonon contributions. As we are interested in studying the change in the direct gap,  $k$  is taken to be zero.

The calculated band-gap change as a function of  $T$  in GaAs and  $Hg_{0.78}Cd_{0.22}Te$  is shown in Figs. 1 and 2, respectively. With increasing  $T$ , the direct gap decreases in GaAs but increases in  $Hg_{0.78}Cd_{0.22}Te$ . Notice that, in both cases, the calculated values are typically within 10 to 15 meV of experimental values [10,13,16-18]. The cross ( $\times$ ) at  $T=0$  represents the calculated zero-point correction to the gap (-26 meV for GaAs and 10 meV for  $Hg_{0.78}Cd_{0.22}Te$ ). The zero temperature band gap calculated without electron-phonon interactions should have this correction subtracted for comparison them to experimental values.

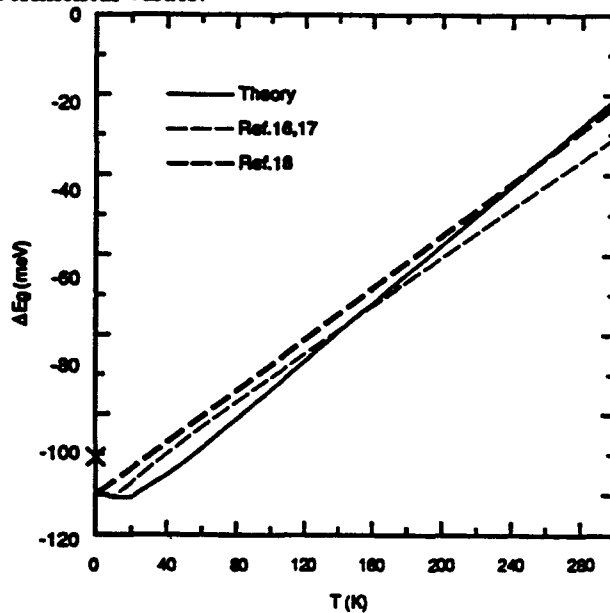
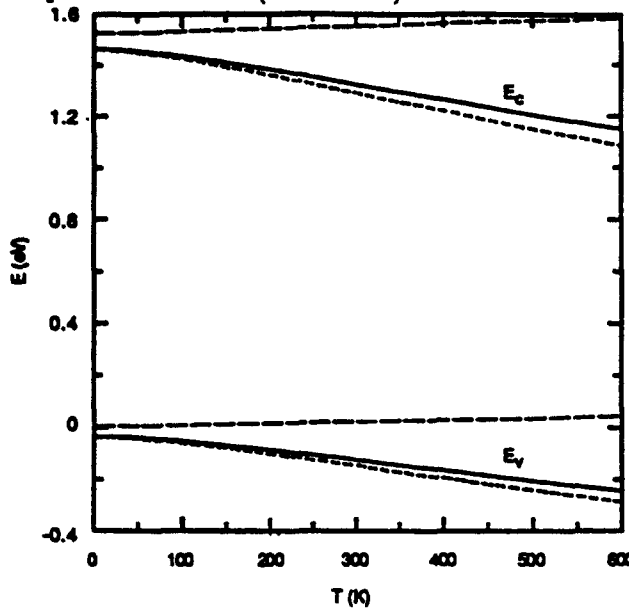


FIG. 2. Change in the band gap of  $Hg_{0.78}Cd_{0.22}Te$  with temperature.

The change in the gap is traditionally explained in terms of inter- and intraband interactions. The intravalance (conduction) band interactions push the valence (conduction) band edge up (down), thus reducing the gap. Similarly, the valence-conduction band interactions increase the gap. Hence one might expect the gap to decrease in wide-gap semiconductors and possibly increase in small-gap semiconductors. In addition, arguments based only on total density of states and ignoring variations in matrix elements will predict both the conduction band edge  $E_c$  and the valence band edge  $E_v$  move up in energy, particularly in small-gap materials, because the hole effective mass is one to two orders of magnitude larger than the electron mass. As seen from Fig. 3, our

**FIG. 3.** Variation of conduction and valence band edges (solid lines) with temperature. Interaction with valence bands pushes the states up (dashed lines) and that with conduction bands pushes them down (dotted lines).



detailed calculations do not support this traditional view. We find that both  $E_c$  and  $E_v$  (solid lines) move down in energy. This trend is observed in all semiconductors tried (InP, InAs, InSb, HgCdTe alloys, InTlP alloys, and GaSb). The movement of the band edges due to interaction with valence bands (dashed lines) and that with conduction bands (dotted lines) is also shown in Fig. 3. We see that interaction of the band edges with the conduction bands (CBs) is much stronger than with valence bands (VBs), and consequently both  $E_v$  and  $E_c$  move down in energy.

**TABLE I.** Calculated change at 300 K in the valence (v) and conduction (c) band edge energies in meV. Contributions from interaction with various phonon modes are shown in the third through tenth rows.

band	1	2	3	4	5	6	7	8	
Total	v	0.3	3.0	9.4	9.7	-36.4	-37.9	-42.5	-30.3
	c	0.7	1.8	13.1	18.6	-97.0	-33.8	-68.3	-36.2
	v	0.2	1.8	6.8	4.8	-23.7	-27.3	-30.0	-15.9
TA	c	0.4	0.6	11.0	16.4	-11.5	-15.0	-52.0	-14.2
	v	0.0	0.6	0.4	1.5	-6.9	-3.1	-2.7	-5.4
LA	c	0.2	0.7	0.7	0.6	-62.2	-10.1	-1.7	-8.5
	v	0.0	0.4	1.8	2.9	-3.3	-6.3	-5.5	-3.8
TO	c	0.0	0.1	1.1	1.4	-5.4	-5.2	-12.9	-9.2
	v	0.0	0.2	0.5	0.6	-2.5	-1.2	-4.4	-5.3
LO	c	0.1	0.3	0.3	0.2	-18.0	-3.5	-1.7	-4.3

We analyze the strength of inter- and intraband electron-phonon interactions by presenting the contributions from each band and from each phonon mode. Table I lists the calculated values for GaAs at 300 K. Although spin is included in our band structure calculations, only spin averaged values are listed. Band indices 1 to 4 correspond to VBs, and the others to CBs. The first two rows show changes in  $E_v$  and  $E_c$  due to interactions with various bands. Contributions from each phonon mode are listed in the remaining rows. The lowest VB is about 13 to 15 eV below  $E_v$  and  $E_c$ , and hence the interaction impacts the band edges only very little. This band could be omitted without much loss of accuracy. We see that the interaction with other VBs is also generally weak and the matrix elements connecting VB states are always found to be small. However, interaction of the band edges with CBs is very strong and negative. Particularly, the interaction of  $E_c$  with the lowest conduction band is strong because of a combination of large matrix elements and small energy denominators [Eq. (1)]. As  $E_c$  moves down more than  $E_v$ , the gap narrows in GaAs. To understand the role of various phonons, we display the contribution from each mode separately. The calculated values of change in the band edges at 300 K in GaAs are listed in the third through tenth rows of the table. While the conduction band edge-CB interaction mediated by optical phonons contribute modestly to the value of  $E_c$ , we see that acoustic phonons account for about 75% of the total change in the valence and conduction band edge energies.

Our calculations for  $Hg_{0.78}Cd_{0.22}Te$  alloy show a qualitatively similar role for phonons. However, we find that  $E_v$  moves down more, because of the narrow-gap (100 meV), than  $E_c$  and that the gap increases with temperature. Then we treated InSb and  $Hg_{0.70}Cd_{0.30}Te$ . Although they both have the same zero temperature gap of 0.235 eV, the InSb gap decreases with T, whereas the  $Hg_{0.70}Cd_{0.30}Te$  gap increases with T. The difference is mainly because of the lowest conduction band width and the intervalley separation. In the HCT alloy, the  $\Gamma$  and the next nearest valley L are separated by 2.7 eV whereas that energy separation is only 0.7 eV in InSb. The smaller energy denominator [Eq. (1)] in the interaction of the conduction band edge with the lowest conduction band pushes down  $E_c$  much more in InSb than in  $Hg_{0.70}Cd_{0.30}Te$ , and consequently the gap decreases in InSb. Of course, for a larger Cd concentration the zero T gap is also larger, and  $E_v$  moves down by only a small amount and the finite temperature gap starts to decrease. The combination of gap size, the lowest conduction band width, and intervalley separation gives rise to these interesting variations in the gap with T.

The observation that both  $E_v$  and  $E_c$  move down in energy has an important effect on band offsets in heterojunction-based devices. For example, the zero temperature valence band offset between  $Hg_{0.78}Cd_{0.22}Te$

and CdTe is believed to be around 350 meV. However, we find that at 300 K,  $E_v$  in  $Hg_{0.78}Cd_{0.22}Te$  and in CdTe moves down by 215 meV and 30 meV, respectively. If the dipole contribution remains the same, the valence band offset decreases to 165 meV at 300 K. In addition to the electron-phonon interactions discussed above, lattice dilation changes the band edges differently [9]. In my case, this band offset change has enormous influence on the design of IR absorption and lasing devices.

In addition to GaAs and  $Hg_{0.78}Cd_{0.22}Te$ , we studied the band-gap variation with temperature in InAs, InP, InSb, GaSb, and CdTe compounds. The calculations produced correct trends in all these compounds, and the values in InP, GaSb, and CdTe are in fairly good agreement with experiments. However, the calculated changes in the band gap of InAs and InSb were about a factor of 1 smaller than in the experiments. We find that our calculated TA phonon frequencies away from zone center in these compounds were considerably larger than in experiments. As noted from Table I, a substantial contribution comes from acoustic phonons. Consequently, our theoretical values of  $E_g(T)$  are smaller than in experiments. Although these inaccuracies do not change the conclusions of this Letter, better predictability should result from improvement in the dynamical matrix calculated from the underlying Hamiltonian. In addition, at higher temperatures higher-order perturbation terms must be included along with finite temperature 'renormalized' bands rather than the zero temperature bands. Such renormalization affects the monotonic change in the gap and introduces nonlinear terms.

In summary, we have calculated temperature variations of band gaps in various semiconductors. A fairly accurate HTB Hamiltonian is used in the calculation of electron and phonon structures. The calculations explain the increase in the band gap of  $Hg_{0.78}Cd_{0.22}Te$ , and the decrease in the band gap of GaAs, and show that acoustic phonons make the major contribution. Contrary to traditional thinking based on total density of states arguments, we find that both valence and conduction band edges move down in energy. One important consequence of this observation will be in the band offsets in semiconductor heterojunction devices. Finally, there is a small and always negligible zero-point motion contribution to low-temperature band gaps arising from electron-phonon interactions.

We thank Dr. M. Cardona of the Max Planck Institute, Stuttgart, for pointing us to several references. Funding from ONR (contract N00014-93-C-0091) and AFPA (contract MDA972-92-C-0053) is gratefully acknowledged.

- [1] Y. P. Varshini, *Physica* **34**, 149 (1967).
- [2] V. Heine and J. A. Van Vechten, *Phys. Rev. B* **13**, 1622 (1976).
- [3] P. B. Allen and V. Heine, *J. Phys. C* **9**, 2305 (1976).
- [4] P. B. Allen and M. Cardona, *Phys. Rev. B* **27**, 4760 (1983).
- [5] S. Gopalan, P. Lautenschlager, and M. Cardona, *Phys. Rev. B* **35**, 5577 (1987).
- [6] M. Cardona and S. Gopalan, in *Progress on electron properties of solids*, R. Girlanda et al., eds. (Kluwer Academic publishers, 1989), p. 52.
- [7] R. D. King-Smith, R. J. Needs, V. Heine, and M. J. Hodgson, *Europhys. Lett.* **10**, 569 (1989).
- [8] S. Zollner, S. Gopalan, and M. Cardona, *Sol. State Comm.* **77**, 485 (1991).
- [9] K. J. Malloy and J. A. Van Vechten, *J. Vac. Sci. Technol. B* **9**, 2112 (1991).
- [10] P. Lautenschlager, M. Garriga, S. Logothetidis, and M. Cardona, *Phys. Rev. B* **35**, 9174 (1987); and references cited therein.
- [11] Z. Hang, D. H. Pollak, G. D. Pettit, and M. Woodall, *Phys. Rev. B* **44**, 10546 (1991).
- [12] L. Pavisi, F. Piazza, A. Rudra, J. F. Carlin, and M. Illegems, *Phys. Rev. B* **44**, 9052 (1991).
- [13] E. Grilli, M. Guzzi, R. Zamboni, and L. Pavesi, *Phys. Rev. B* **45**, 1638 (1992).
- [14] P. Y. Liu and J. C. Maan, *Phys. Rev. B* **47**, 16274 (1993).
- [15] M. E. Allali, C. B. Sorenson, E. Veje, and P. T. Petersson, *Phys. Rev. B* **48**, 4398 (1993).
- [16] G. L. Hansen, J. L. Schmit, and T. N. Casselman, *J. Appl. Phys.* **53**, 7099 (1982).
- [17] D. G. Seiler, J. R. Lowney, C. L. Littler, and M. R. Loloee, *J. Vac. Sci. Technol. A* **8**, 1237 (1990).
- [18] J. C. Brice, *Properties of mercury cadmium telluride*, J. Brice and P. Capper, eds. (EMIS datareviews series 3, INSPEC publication, 1987), p. 105.
- [19] Landolt-Börnstein *Numerical data and functional relationships in science and technology*, Madelung, Schultz and Weiss (eds.), New series, Vol. 17 (1982).
- [20] A. -B. Chen and A. Sher, *Phys. Rev. B* **23**, 5360 (1981).
- [21] S. Krishnamurthy, A. -B. Chen, and A. Sher, *J. Appl. Phys.* **63**, 4540 (1988).
- [22] S. Krishnamurthy, A. Sher, and A. -B. Chen, *Phys. Rev. Lett.*, **64**, 2531 (1990); *Appl. Phys. Lett.* **55**, 1002 (1989); *Appl. Phys. Lett.* **52**, 468 (1988).
- [23] S. Krishnamurthy, A. Sher, and A. -B. Chen, *Appl. Phys. Lett.* **53**, 1853 (1988).
- [24] W. Harrison, *Electronic structure and properties of solids* (Freeman, San Francisco, 1980).
- [25] S. Krishnamurthy and M. Cardona, *J. Appl. Phys.* **74**, 2117 (1993).
- [26] R. M. Martin, *Phys. Rev. B* **1**, 4005 (1970).